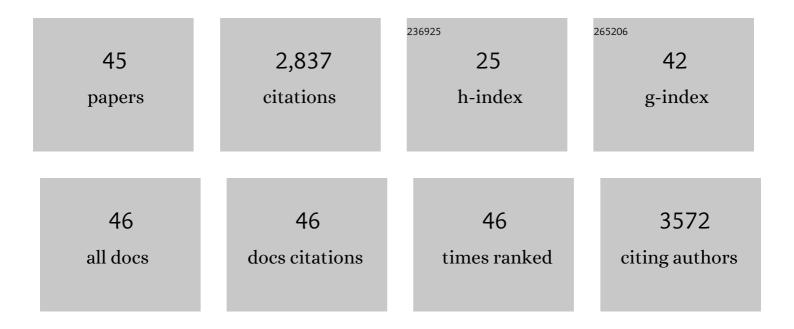
Hao Jin

List of Publications by Year in descending order

Source: https://exaly.com/author-pdf/4913847/publications.pdf Version: 2024-02-01



ΗλΟΙΙΝ

#	Article	IF	CITATIONS
1	Lightweight and Anisotropic Porous MWCNT/WPU Composites for Ultrahigh Performance Electromagnetic Interference Shielding. Advanced Functional Materials, 2016, 26, 303-310.	14.9	697
2	Thin and flexible multi-walled carbon nanotube/waterborne polyurethane composites with high-performance electromagnetic interference shielding. Carbon, 2016, 96, 768-777.	10.3	301
3	Microstructure Design of Lightweight, Flexible, and High Electromagnetic Shielding Porous Multiwalled Carbon Nanotube/Polymer Composites. Small, 2017, 13, 1701388.	10.0	163
4	Synergistic effects from graphene and carbon nanotubes endow ordered hierarchical structure foams with a combination of compressibility, super-elasticity and stability and potential application as pressure sensors. Nanoscale, 2015, 7, 9252-9260.	5.6	126
5	Buckled AgNW/MXene hybrid hierarchical sponges for high-performance electromagnetic interference shielding. Nanoscale, 2019, 11, 22804-22812.	5.6	106
6	Low-voltage and high-performance electrothermal actuator based on multi-walled carbon nanotube/polymer composites. Carbon, 2015, 84, 327-334.	10.3	105
7	Structure, Optical, and Catalytic Properties of Novel Hexagonal Metastable <i>h</i> -MoO ₃ Nano- and Microrods Synthesized with Modified Liquid-Phase Processes. Chemistry of Materials, 2010, 22, 6202-6208.	6.7	99
8	Thermal Transport in the Hidden-Order State of URu2Si2. Physical Review Letters, 2005, 94, 156405.	7.8	89
9	Mechanically robust ANF/MXene composite films with tunable electromagnetic interference shielding performance. Composites Part A: Applied Science and Manufacturing, 2020, 135, 105927.	7.6	85
10	Tuning the Interfacial Mechanical Behaviors of Monolayer Graphene/PMMA Nanocomposites. ACS Applied Materials & Interfaces, 2016, 8, 22554-22562.	8.0	84
11	Mechanical behavior and properties of hydrogen bonded graphene/polymer nano-interfaces. Composites Science and Technology, 2016, 136, 1-9.	7.8	80
12	Broadband composite radar absorbing structures with resistive frequency selective surface: Optimal design, manufacturing and characterization. Composites Science and Technology, 2017, 145, 10-14.	7.8	80
13	Thermoelectricity ofURu2Si2: Giant Nernst effect in the hidden-order state. Physical Review B, 2004, 70,	3.2	73
14	Synergistic effect of a r-GO/PANI nanocomposite electrode based air working ionic actuator with a large actuation stroke and long-term durability. Journal of Materials Chemistry A, 2015, 3, 8380-8388.	10.3	56
15	Three-dimensional Sponges with Super Mechanical Stability: Harnessing True Elasticity of Individual Carbon Nanotubes in Macroscopic Architectures. Scientific Reports, 2016, 6, 18930.	3.3	56
16	Hierarchical Grapheneâ€Based Films with Dynamic Selfâ€Stiffening for Biomimetic Artificial Muscle. Advanced Functional Materials, 2016, 26, 7003-7010.	14.9	53
17	Thermodynamic properties of Mg2Si and Mg2Ge investigated by first principles method. Journal of Alloys and Compounds, 2010, 499, 68-74.	5.5	52
18	Ultra-broadband frequency responsive sensor based on lightweight and flexible carbon nanostructured polymeric nanocomposites. Carbon, 2017, 121, 490-501.	10.3	46

Hao Jin

#	Article	IF	CITATIONS
19	Creep-resistant behavior of MWCNT-polycarbonate melt spun nanocomposite fibers at elevated temperature. Polymer, 2013, 54, 3723-3729.	3.8	45
20	An experimental apparatus for simultaneously measuring Seebeck coefficient and electrical resistivity from 100 K to 600 K. Review of Scientific Instruments, 2013, 84, 043903.	1.3	44
21	Flexible and easy-to-tune broadband electromagnetic wave absorber based on carbon resistive film sandwiched by silicon rubber/multi-walled carbon nanotube composites. Carbon, 2017, 121, 544-551.	10.3	42
22	Theoretical study on thermoelectric properties of Mg2Si and comparison to experiments. Computational Materials Science, 2012, 60, 224-230.	3.0	39
23	Ultrafast response of spray-on nanocomposite piezoresistive sensors to broadband ultrasound. Carbon, 2019, 143, 743-751.	10.3	33
24	Nanostructured carbon materials based electrothermal air pump actuators. Nanoscale, 2014, 6, 6932-6938.	5.6	32
25	Multifunctional Polymer-Based Graphene Foams with Buckled Structure and Negative Poisson's Ratio. Scientific Reports, 2016, 6, 32989.	3.3	31
26	Can insulating graphene oxide contribute the enhanced conductivity and durability of silver nanowire coating?. Nano Research, 2019, 12, 1571-1577.	10.4	29
27	Low-Temperature Thermoelectric Properties of β-Ag2Se Synthesized by Hydrothermal Reaction. Journal of Electronic Materials, 2011, 40, 624-628.	2.2	26
28	A coatable, light-weight, fast-response nanocomposite sensor for the <i>in situ</i> acquisition of dynamic elastic disturbance: from structural vibration to ultrasonic waves. Smart Materials and Structures, 2016, 25, 065005.	3.5	25
29	Rigid vortices in MgB2. Applied Physics Letters, 2003, 83, 2626-2628.	3.3	23
30	A temperature-activated nanocomposite metamaterial absorber with a wide tunability. Nano Research, 2018, 11, 3931-3942.	10.4	22
31	Graphene-based nanocomposite strain sensor response to ultrasonic guided waves. Composites Science and Technology, 2019, 174, 42-49.	7.8	21
32	Evidence for a New Magnetic Field Scale inCeCoIn5. Physical Review Letters, 2006, 96, 077207.	7.8	14
33	Study of the transport properties of La1.85â^'xSr0.15+xCu1â^'xMxOy (M = Fe, Ga). Physics Letters, Section A: General, Atomic and Solid State Physics, 1998, 249, 153-159.	2.1	13
34	Thermal transport property of Ge ₃₄ and d-Ge investigated by molecular dynamics and the Slack's equation. Chinese Physics B, 2010, 19, 076501.	1.4	11
35	Atomistic simulation of Si–Ge clathrate alloys. Chemical Physics, 2008, 344, 299-308.	1.9	9
36	Structure and transport properties of Cr doped La214 system. Physica C: Superconductivity and Its Applications, 1999, 314, 263-268.	1.2	7

Hao Jin

#	Article	IF	CITATIONS
37	Upper Critical Field and Irreversibility Line Determined by Transport Measurement of the New Superconductor MgB 2. Chinese Physics Letters, 2001, 18, 823-825.	3.3	6
38	Effective fabrication of flexible negative refractive index metamaterials using a simple screen printing method. Journal of Materials Chemistry C, 2017, 5, 5378-5386.	5.5	6
39	Magnetic relaxation in high-temperature superconductors. Physics Letters, Section A: General, Atomic and Solid State Physics, 1999, 255, 183-186.	2.1	4
40	Crystal structure and transport properties of La1.75Sr0.25Cu0.9M0.1O4 (M=Cr, Mn, Fe, Co, Ga and Al). Physica C: Superconductivity and Its Applications, 1999, 315, 124-128.	1.2	2
41	Argument forE ×j relation of high temperature superconductors. Science in China Series A: Mathematics, 2000, 43, 163-170.	0.5	1
42	Vortex-unbinding and finite-size effects inTl2Ba2CaCu2O8thin films. Physical Review B, 2003, 68, .	3.2	1
43	Kondo effect induced suppression of superconductivity in Y1â^'xPrxBa2Cu3O7â^'Î′. Physica C: Superconductivity and Its Applications, 1997, 282-287, 1395-1396.	1.2	0
44	E - j relation in the vortex-liquid region of high temperature superconductors. Physica C: Superconductivity and Its Applications, 2000, 341-348, 1309-1310.	1.2	0
45	Reargument over E â^1⁄4 j relation of high temperature superconductors. Science in China Series A: Mathematics, 2001, 44, 513-527.	0.5	0